

# Academic Journal of Chemistry

ISSN(e): 2519-7045

Vol. 2, No. 1, pp: 1-7, 2017

URL: <http://arpweb.com/?ic=journal&journal=20&info=aims>

## Preparation, Characterization and Flame Retardancy of Expandable Graphite Modified By Ferric Hydroxide. Part II—Flame Retardation and Its Interaction with Ammonium Polyphosphate for Polyethylene

Xiu-yan Pang\*

College of Chemistry and Environmental Science, The Flame Retardant Material and Processing Technology Engineering Technology Research Center of Hebei Province, Hebei University, Baoding 071002, China

Wei-shu Chang

College of Chemistry and Environmental Science, The Flame Retardant Material and Processing Technology Engineering Technology Research Center of Hebei Province, Hebei University, Baoding 071002, China

**Abstract:** The influence of expendable graphite ( $EG_{Fe}$ ) modified by ferric hydroxide and its interaction with ammonium polyphosphate (APP) on combustion behavior and thermal stabilities of linear low density polyethylene (LLDPE) were investigated. Results showed  $EG_{Fe}$  presented better flame retardation than the normal expandable graphite (EG). A 30 wt%  $EG_{Fe}$  improved the limiting oxygen index (LOI) of LLDPE from 17.6% to 28.1%. Furthermore, the combination between  $EG_{Fe}$  and APP improved the LOI of 70LLDPE/20APP/10 $EG_{Fe}$  to 31.6%, and the vertical combustion UL-94 level reached V-0.  $EG_{Fe}$  and APP were both beneficial for the improvement of composite thermal stabilities, and there was synergistic performance between them which had been testified by the LOI results. Union between  $EG_{Fe}$  and APP was of benefit for the formation of continuous and compact char layers, which makes 70LLDPE/20APP/10 $EG_{Fe}$  composite show better flame retardation than the independent 70LLDPE/30APP or 70LLDPE/30 $EG_{Fe}$  composite.

**Keywords:** Modified expandable graphite; Ferric hydroxide; Interaction; Ammonium polyphosphate; Linear low density polyethylene; Residual characteristics.

### 1. Introduction

Flame retardants (FRs) often added to materials to prevent combustion and delay the spread of fire after ignition. In recent years, intumescent flame retardants (IFRs) have attracted much attention not only because they are more environmentally friendly than halogenated flame retardants (HFRs) [1], but also they are more efficient than inorganic FRs [2, 3]. When heating IFR, it will form a foamed cellular charred layer on the surface of the substrate, which decelerates heat and mass transfer between the gaseous and condensed phases [4]. Ammonium polyphosphate (APP) is an effective IFR for polymer materials [5, 6], and its efficiency is generally attributed to the increase in the char formation through involving in altering the pathway of the thermal degradation of the substrate and promoting solid-state reaction leading to carbonization [7]. However, the flame retardation of APP for polyolefin is very limited due to the absence of oxygenous groups in matrix and resulting in the insufficient protective layer [8].

Expandable graphite (EG) is another kind of IFR. It can play multiple roles such as char-forming agent, blowing agent and smoke suppressant [9]. When heating the EG, it will instantly expand and release noncombustible  $H_2O$  and  $CO_2$  gases to dilute the concentration of the volatile flammable compositions. At the same time, the flake EG particles turn into swollen “graphite worms”, which causes protection for matrix surface from the covered multicellular char. Due to its outstanding capability, EG has been used in the flame retardance of polymer materials [10, 11]. Whereas, there are some problems need to be solved. On the one hand, EG is normally prepared with  $H_2SO_4$  as intercalation agent and  $H^+$  donor [12], which may result in the high sulfur content in product and the release of  $SO_2$  coming from the oxidation reaction between  $H_2SO_4$  and graphite atom. At the same time, the formed multicellular “graphite worms” chars are loose and easy to collapse and even flow away under the influence of flame pressure or heat convection, which leads to the loss of residual char and decreases the efficiency in slowing down heat and mass transfer. It is important to improve EG efficiency and environmental friendliness at the same time.

Therefore, the graphite intercalation reaction requires improvement, or the normal EG needs modification. Firstly, some assistant intercalators such as nitric acid, oxalic acid, acetic anhydride can replace a part of  $H_2SO_4$  [13, 14]. EG intercalated by  $H_2SO_4$ /silicate indicated an expandable volume (EV) of 517 mL/g and limited oxygen index (LOI) value of 28.7% for ethylene vinyl acetate [15]. It was higher than that of the single  $H_2SO_4$  intercalated EG

\*Corresponding Author

with an EV of 433 mL/g and LOI value of 24.4% respectively. EG can also get excellent property through its outside surface modification by binding, chemical bonding and sol-gel hydrolysis precipitation methods. The titania nanocrystals in EG could be prepared using organically modified silicate as a binder [15]. The EG prepared using chemical bonding method with silane coupling agent and boric acid presented improved flame retardancy for rigid polyurethane foam [16]. An anatase  $\text{TiO}_2$ /EG with high expansion volume was prepared through sol-gel process with titania gel introduced to EG surface [17].

Addition of EG together with APP has been testified to be an efficient method in improving flame retardancy through enhancing the continuous, compact of residue layers [18]. Furthermore, as one of transition metal oxides,  $\text{Fe}_2\text{O}_3$  can be used as FR for its smoke suppression [19]. It can also obviously impact on the thermal decomposition process of APP through accelerating the release of  $\text{NH}_3$  and  $\text{H}_2\text{O}$  in the earlier period and increasing the high temperature residue in the later period for the formation of metallic phosphate. Basing on the reasons of (1) the independent flame retardation of EG, APP and  $\text{Fe}_2\text{O}_3$ , (2) the improvement of  $\text{Fe}_2\text{O}_3$  for EG and APP flame retardancy and (3) the synergistic effect between APP and EG [20], the purpose of this research was to prepare a ferric hydroxide modified EG (written as  $\text{EG}_{\text{Fe}}$ ). Flame retardancy of the  $\text{EG}_{\text{Fe}}$ , the referenced EG (intercalated by  $\text{H}_2\text{SO}_4$ ), APP and APP/ $\text{EG}_{\text{Fe}}$  for LLDPE were all tested. LOI and vertical burning UL-94 tests, thermal gravimetric and differential thermal gravimetric (TG/DTG) analyses were performed to evaluate flame retardant performance and the thermal stability. Digital camera and scanning electron microscope (SEM) were employed to observe the residual char morphology. In the literature available, there is little investigation on the combustion behavior and interaction of APP with the modified  $\text{EG}_{\text{Fe}}$  for LLDPE.

## 2. Experimental

### 2.1. Materials and Sample Preparation

Natural flake graphite (average particle size of 0.30 mm, carbon content of 96 wt%) was provided by Xite Carbon CO. LTD, Qingdao, China. LLDPE (920NT(EGF-34), melt index 1.0 g/10 min) was purchased from Sinopec Sabic Tianjin Petrochemical.  $\text{FeCl}_3 \cdot 6\text{H}_2\text{O}$ ,  $\text{KMnO}_4$ ,  $\text{NH}_3 \cdot \text{H}_2\text{O}$  (25 wt%) and  $\text{H}_2\text{SO}_4$  (98 wt%) were all analytical agents and used as received.

### 2.2. Preparation of the EG

The EG with  $\text{H}_2\text{SO}_4$  as intercalator was prepared according to the mass ratio graphite (C): $\text{H}_2\text{SO}_4$  (75 wt %): $\text{KMnO}_4$  of 1.0:6.67:0.15. Its initial expansion temperature and EV are 200°C and 530 mL/g respectively.

### 2.3. Preparation of the $\text{EG}_{\text{Fe}}$

The mass ratio of  $\text{FeCl}_3$  to EG was 0.1:1, dosage of  $\text{NH}_3 \cdot \text{H}_2\text{O}$  with a wt% of 25% was controlled as 0.4 mL, hydrolysis precipitation reaction lasted 2.5 h at room temperature, and the  $\text{EG}_{\text{Fe}}$  drying temperature was 100°C. The obtained  $\text{EG}_{\text{Fe}}$  shows an initial expansion temperature of 168°C and EV of 554 mL/g. Results of FTIR, SEM and XRD testify hydrolysis precipitation reaction between EG and  $\text{FeCl}_3$  produces the  $\text{EG}_{\text{Fe}}$ , and the final existence form of  $\text{FeCl}_3$  is  $\text{Fe(OH)}_3$ , which covers on the outside surface of EG.

### 2.4. Preparation of the Flame Retarded LLDPE Composites

FR were added into melted LLDPE at 120°C in Muller at a 30 wt% dosage, then the mixtures were pressed at 125°C and 10 MPa, and chopped into slivers with two different sizes of 120.0×6.0×3.0 mm<sup>3</sup> and 127.0×13.0×3.0 mm<sup>3</sup> for the evaluation of LOI and vertical combustion level.

### 2.5. Characterization of the Samples

A TM3000 SEM (Japan) was applied to observe residue structure and morphology of the flame retarded LLDPEs after their combustion tests, and the FTIR spectra were recorded between 4000-400 cm<sup>-1</sup> using a FTIR spectrometer (Nicolet 380, America Thermo Electron Corporation) with a resolution of 2 cm<sup>-1</sup>.

The incised slivers with a size of 120.0×6.0×3.0 mm<sup>3</sup> were used to measure LOI according to Standard of GB/T2406-1993 with oxygen index instrument (Chengde, China). The vertical combustion test was performed using a HC-3 vertical burning instrument (Tientsin, China) on sheets with a size of 127.0×13.0×3.0 mm<sup>3</sup> as per the standard UL 94-1996.

In TG/DTG analysis (STA 449C, Germany), about 5.0 mg sample, laid in porcelain crucible, was detected under  $\text{N}_2$  atmosphere with a flux of 25 mL/min. It was heated in the range of 40-800°C at a heating rate of 10°C/min. Changes of sample weight as temperature were recorded.

## 3. Results and Discussion

### 3.1. Combustion Behavior

The combustion behaviors of LLDPE loading with different kinds and doses of RFs were evaluated in LOI and vertical combustion UL-94 tests, and the results were showed in Table 1. LLDPE is very flammable with a LOI of 17.6%, and the combustion accompanies with serious melt-dripping as showed in Figure 1 (a). While, the addition of the tested FRs can all affect combustion process. Noticeably, addition of the EG at 30 wt% leads LOI value of the

70LLDPE/30EG composite to 25.0%, and the UL-94 level to V-1. Addition of the same amount of EG<sub>Fe</sub> can not only improve the UL-94 level to V-0, but also increase the LOI value to 28.1%. The results indicate loading of Fe(OH)<sub>3</sub> enhances the flame retardation of EG<sub>Fe</sub> for LLDPE. The improved UL-94 level should be attributed to the protective intumescence carbonaceous char formed on 70LLDPE/30 EG<sub>Fe</sub> polymer surface as showed in [Figure 1 \(b\)](#).

The independent APP presents a weak efficiency for LLDPE, LOI value of the 70LLDPE/30APP specimen is only 19.9%, and accompanied by serious melt-dropping and ignition. While, additions of EG<sub>Fe</sub> and APP at different wt% can not only increase the LOI value, but also all improve the UL-94 level to V-0 simultaneously. Meanwhile, these LOI values are all obviously higher than the theoretical results of LOI<sub>the</sub> calculated according to their wt% in composite and independent LOI value [\[19\]](#). Therefore, it can be inferred that there is synergistic efficiency between these two FRs. Meanwhile, the APP/EG<sub>Fe</sub> ratio has an important influence on flame retardancy, and the tested optimum mass ratio is 2:1 as showed in 70LLDPE/20APP/10EG<sub>Fe</sub>, the LOI and UL-94 level can reach 30.5% and V-0 respectively. The well flame retardancy comes from the protection of intumescence carbonaceous char jointly provided by APP and EG<sub>Fe</sub> as showed in [Figure 1 \(c\)](#).

**Table-1.** The LOI values and UL-94 results of the flame retarded LLDPE composites <sup>a</sup>

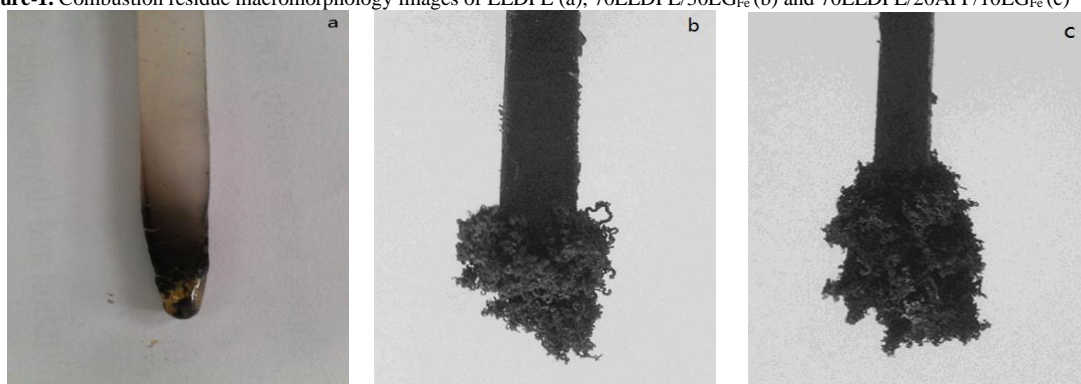
Samples	LOI % LOI <sub>exp</sub>	LOI <sub>the</sub>	UL-94 level
100 LLDPE	17.6	N.D.	N.D.
70 LLDPE/30EG	25.0	N.D.	V-1
70 LLDPE/30 EG <sub>Fe</sub>	28.1	N.D.	V-0
70 LLDPE/30APP	19.9	N.D.	N.D.
70LLDPE/10APP/20 EG <sub>Fe</sub>	29.1	25.4	V-0
70LLDPE/15APP/15 EG <sub>Fe</sub>	30.2	24.1	V-0
70LLDPE/20APP/10 EG <sub>Fe</sub>	31.6	22.7	V-0

<sup>a</sup> LOI<sub>exp</sub>: the LOI value detected in experiments.

LOI<sub>the</sub>: the LOI value calculated according to FRs wt% in composite and their independent LOI value.

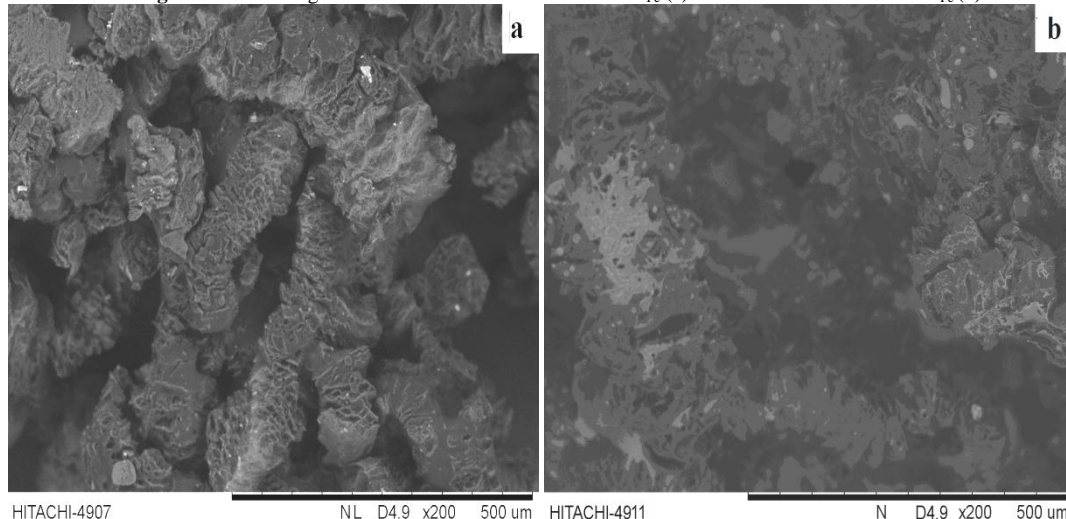
N.D.: the data is inexistence, or it can not be detected.

**Figure-1.** Combustion residue macromorphology images of LLDPE (a), 70LLDPE/30EG<sub>Fe</sub> (b) and 70LLDPE/20APP/10EG<sub>Fe</sub> (c)



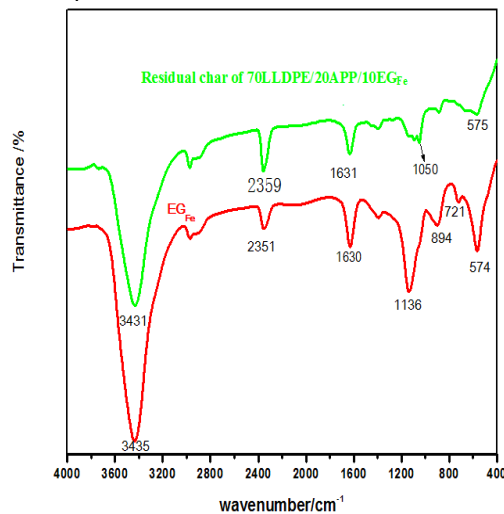
### 3.2. The Combustion Residue Micromorphology

The residual char micromorphology has important influence on flame retardation. Therefore, residual incision of 70LLDPE/30EG<sub>Fe</sub> and 70LLDPE/20APP/10EG<sub>Fe</sub> after their combustion experiments are recorded by SEM. As showed in [Figure 2\(a\)](#), a regular and discontinuous "open-cellular" structure on the surface is observed in 70LLDPE/30EG<sub>Fe</sub> due to the expansion of EG<sub>Fe</sub> (showing the "popcorn effect"), originating from the released gases in redox reaction between residual H<sub>2</sub>SO<sub>4</sub> and the graphite. It's the discontinuity that causes the composite easy breaking, and the tensile strength is detected only 5.17 MPa. The residue incision of 70LLDPE/20APP/10EG<sub>Fe</sub> showed in [Figure 2 \(b\)](#) is relatively continuous and compact due to the conglutination of APP decomposition products, and the tensile strength indicates as 7.54 MPa; this structure can suppress the mentioned "popcorn effect" to a certain extent, and then provide a good shield that insulates the substrate from radiant heat. It is the continuous and compact residual that makes 70LLDPE/20APP/10EG<sub>Fe</sub> composite show well flame retardancy than the independent APP or EG<sub>Fe</sub> flame retarded composite.

**Figure-2.** SEM images of residual char of 70LLDPE/30EG<sub>Fe</sub> (a) and 70LLDPE/20APP/10EG<sub>Fe</sub> (b)

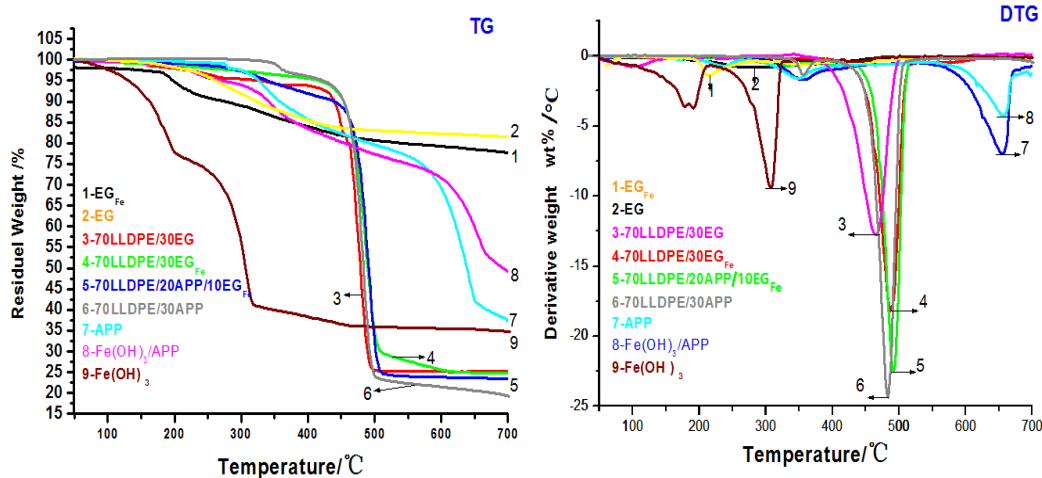
### 3.3. FTIR Analysis of LLDPE Residues

The chemical composition and functional groups of the 70LLDPE/20APP/10EG<sub>Fe</sub> combustion residue was obtained from FTIR analysis and contrastively showed in [Figure 3](#). The characteristic stretching vibrations absorption peaks of -OH ( $3448\text{ cm}^{-1}$ ) and C=C ( $1630\text{ cm}^{-1}$ ) can be observed caused by the remainder of EG<sub>Fe</sub> and LLDPE. Peaks round of  $2350\text{ cm}^{-1}$  are stretching vibrations absorption O-C-O. Compared with the EG<sub>Fe</sub>, the strong stretching vibration absorption of sulphate at about  $1130\text{ cm}^{-1}$  and the bending vibration absorption of Fe-O-H at  $890\text{ cm}^{-1}$  all disappear, but there are obvious superimposed peaks round  $1050\text{ cm}^{-1}$  in the FTIR of 70LLDPE/20APP/10EG<sub>Fe</sub>, it is because the absorption peak of S=O and P=O are both appear in the range of  $1080\text{-}1300\text{ cm}^{-1}$  [19]. The characteristic absorption of the Fe-O at  $575\text{ cm}^{-1}$  presents both in EG<sub>Fe</sub> and 70LLDPE/20APP/10EG<sub>Fe</sub>. The results indicate combustion reaction has transferred Fe(OH)<sub>3</sub> to Fe<sub>2</sub>O<sub>3</sub>, and Fe<sub>2</sub>O<sub>3</sub>, APP decomposition product mainly exist in condensed phase.

**Figure-3.** FTIR spectra of EG<sub>Fe</sub> and residual char of 70LLDPE/20APP/10EG<sub>Fe</sub>

### 3.4. Thermal Property of the Flame Retarded LLDPE Composites

Thermal stability of flame retarded LLDPE is related to the addition of FRs. TG/DTG analysis for 70LLDPE/30EG, 70LLDPE/30EG<sub>Fe</sub>, 70LLDPE/30APP, 70LLDPE/20APP/10EG<sub>Fe</sub> composites and FRs including EG, EG<sub>Fe</sub>, APP, Fe(OH)<sub>3</sub>, and mixture of Fe(OH)<sub>3</sub>/APP, the results are showed in [Figure 4](#) and [Table 2](#).

**Figure-4.** TG and DTG curves of FRs and LLDPE composites in N<sub>2</sub> atmosphere**Table-2.** Thermoanalysis data of specimens in N<sub>2</sub> atmosphere <sup>b</sup>

Specimens	T <sub>1</sub> /°C	T <sub>5</sub> /°C	T <sub>max</sub> /°C		R <sub>max</sub> / wt% / °C		Residue yield /%	
	I	II	I	II	R <sub>exp</sub>	R <sub>the</sub>		
EG	176	263	277	N.D.	-0.80	N.D.	81.56	N.D.
EG <sub>Fe</sub>	134	208	215	N.D.	-1.38	N.D.	77.73	N.D.
70LLDPE/30EG <sub>Fe</sub>	191	421	488	N.D.	-18.20	N.D.	24.34	N.D.
70LLDPE/30EG	157	328	465	N.D.	-12.77	N.D.	25.17	N.D.
70LLDPE/20APP/10EG <sub>Fe</sub>	240	344	491	N.D.	-22.46	N.D.	23.43	N.D.
70LLDPE/30APP	350	421	483	N.D.	-24.34	N.D.	19.32	N.D.
APP	278	326	360	640	-1.68	-6.98	37.22	N.D.
Fe(OH) <sub>3</sub>	75	130	179	309	-3.57	-9.36	34.80	N.D.
Fe(OH) <sub>3</sub> /APP	169	270	345	658	-1.58	-4.27	49.17	25.63

<sup>b</sup> T<sub>1</sub>, T<sub>5</sub>: temperature corresponding to a 1% and 5% mass loss respectively, °C .T<sub>max</sub>: temperature corresponding to the maximum mass loss rate, °C .R<sub>max</sub>: the maximum mass loss rate, wt%/°C .R<sub>exp</sub>: residue yield detected in TG/DTG experiment, %.R<sub>the</sub>: residue yield calculated according to the independent system residue yield and FR dosage in mixture system, %.

In APP/Fe(OH)<sub>3</sub> mixture, the mass ratio of APP to Fe(OH)<sub>3</sub> is approximately determinated according to the dosage of APP in 70LLDPE/20APP/10EG<sub>Fe</sub> and Fe(OH)<sub>3</sub> in EG<sub>Fe</sub>.

The EG, EG<sub>Fe</sub> and 70LLDPE/30EG, 70LLDPE/30EG<sub>Fe</sub> composites all indicate an obvious one-stage degradation profile. The T<sub>1</sub> (temperature corresponding to a 1% mass loss), T<sub>5</sub> (temperature corresponding to a 5% mass loss) and T<sub>max</sub> (temperature corresponding to the maximum mass loss rate) of EG<sub>Fe</sub> are all less than that of the EG for the weak thermal stability of Fe(OH)<sub>3</sub> in EG<sub>Fe</sub>. Therefore it corresponds to a high R<sub>max</sub> (the maximum mass loss rate) of 1.38 wt%/°C and low final residue yield of 77.73%. Mass loss of the 70LLDPE/30EG and 70LLDPE/30EG<sub>Fe</sub> is relatively obvious than the two additives. When the temperature is below 400°C, it's slight and less than 10%, and then about 60% weight loss occurs in the range of 400-500°C, caused by the decomposition of LLDPE and sufficient oxidation of EG and EG<sub>Fe</sub>. 70LLDPE/30EG<sub>Fe</sub> shows better thermal stability than the 70LLDPE/30EG, indicated by the increased T<sub>1</sub>, T<sub>5</sub> and T<sub>max</sub>. Although 70LLDPE/30EG<sub>Fe</sub> indicates a low final residue yield, its flame retardant efficiency for LLDPE is higher than 70LLDPE/30EG as showed in Table 1. These results indicate the existence of Fe(OH)<sub>3</sub> is beneficial for improvement of flame retardancy caused by the interstitial effect of the Fe<sub>2</sub>O<sub>3</sub> produced in Fe(OH)<sub>3</sub> decomposition reaction. The 70LLDPE/30APP composite shows a two-step degradation profile above 300°C. In the first step (roughly corresponding to 300-400°C), a less than 10% weight loss occurs mainly due to the decomposition of APP and the release of NH<sub>3</sub> and H<sub>2</sub>O. Then, an accelerating mass loss takes place due to further decomposition of LLDPE and APP at second step (approximately corresponding to 500-800°C). The final yield of residual char is only 19.32%. 70LLDPE/20APP/10EG<sub>Fe</sub> composite also shows a one-step weight loss. Although its T<sub>1</sub> and T<sub>5</sub> are lower than that of 70LLDPE/30APP, the T<sub>max</sub> is higher than the two independent flame retarded LLDPE composites. At the same time, the 70LLDPE/20APP/10EG<sub>Fe</sub> presents the highest LOI value and best UL-94 level than all the others as having been tested in combustion experiments. The improved thermal stability and flame retardancy should be caused by the combination of APP and EG<sub>Fe</sub>. Although the final residue yield of 70LLDPE/20APP/10EG<sub>Fe</sub> detected in TG/DTG experiments (R<sub>exp</sub>) is between 70LLDPE/30APP and 70LLDPE/30EG<sub>Fe</sub>, it's higher than the theoretical calculated one (R<sub>the</sub>) of 20.99%. The excellent performance should contribute to its continuous and compact residual char as has been showed in Figure 2. To further illuminate the influence of Fe(OH)<sub>3</sub> on APP thermal stability and their contribution to the 70LLDPE/20APP/10EG<sub>Fe</sub> residue yield, TG/DTG tests severally for APP, Fe(OH)<sub>3</sub> and mixture of APP/Fe(OH)<sub>3</sub>

were carried out. The APP shows a two-step degradation profile above 300°C. In the first step (300-500°C), the evolution products are mainly NH<sub>3</sub>, H<sub>2</sub>O gases and polyphosphoric acids [19], which causes a mass decrease of about 20% with a slow rate. Then, an accelerating mass loss takes place due to the release of the volatile P<sub>2</sub>O<sub>5</sub> at second step (500-700°C), and then reserves a residual yield of 37.22%. Fe(OH)<sub>3</sub> presents poor thermal stability and indicates a two-step weight loss. As showed in Figure 4, the decomposition reaction is basically finished when temperature is above 300°C, and the final residue yield of Fe<sub>2</sub>O<sub>3</sub> is 34.80%. As for APP/Fe(OH)<sub>3</sub>, the mixture approximatively presents a two-step degradation profile. When temperature is below 588°C, the mixture shows a weaker thermal stability than the APP. But when the temperature is higher than this value, it presents an enhanced thermal stability and residual yield. The final residue yield keeps 49.17%, obvious higher than the R<sub>the</sub> of 25.63%, calculated according to the residue yield of independent component and the mass ratio of APP to Fe(OH)<sub>3</sub>. The lower T<sub>1</sub>, T<sub>5</sub>, T<sub>max,I</sub> and higher T<sub>max,II</sub>, final residue yield than APP should be caused by the catalysis of Fe<sub>2</sub>O<sub>3</sub> for APP decomposition reaction, and the reaction between Fe<sub>2</sub>O<sub>3</sub>, polyphosphoric acids, which finally leads to the formation of stable polyphosphate [19]. The above results can provide evidence for the 70LLDPE/20APP/10EG<sub>Fe</sub> holding higher R<sub>exp</sub> than the R<sub>the</sub> due to the formation of polyphosphate.

## 4. Conclusions

The EG<sub>Fe</sub> stepwise prepared with chemical oxidation and hydrolysis precipitation method exhibits better flame retardant behavior for LLDPE than the normal EG. Moreover, the combination of EG<sub>Fe</sub> with APP shows more excellent flame retardation. The produced Fe<sub>2</sub>O<sub>3</sub> can not only impel APP to release NH<sub>3</sub>, H<sub>2</sub>O, and produce polyphosphoric acid at relative low temperature, but also form stable polyphosphate and then improve LLDPE composites thermal stability at high temperature due to the continuous and compact char layers. The interstitial filling of Fe<sub>2</sub>O<sub>3</sub> and polyphosphate together with the conglutination between the loose "graphite worms" by polyphosphoric acid can suppress the "popcorn effect" of expanded graphite. The physical synergy and chemical interaction between the used FRs make 70LLDPE/20APP/10EG<sub>Fe</sub> composite show excellent flame retardation. Comparing residue weight with residual char compaction, the latter plays a more important role in improving thermal stability and flame retardancy.

## Acknowledgements

The authors would like to thank Natural Science Foundation of Hebei Province (No. B2015201028) for financial support. Many thanks for Seedling Project of College of Chemistry and Environmental Science (Hebei University) for financial support.

## References

- [1] Wit, C. A., 2002. "An overview of brominated flame retardants in the environment." *Chemosphere*, vol. 46, pp. 583-624.
- [2] Gao, H. L., Hu, S., Han, H. C., and Zhang, J., 2011. "Effect of different metallic hydroxides on flame-retardant properties of low density polyethylene/melamine polyphosphate/starch composites." *Journal of Applied Polymer Science*, vol. 122, pp. 3263-3269.
- [3] Jiao, C. M., Wang, Z. Z., Chen, X. L., and Hu, Y., 2008. "Synthesis of a magnesium/aluminum/iron layered double hydroxide and its flammability characteristics in halogen-free, flame-retardant ethylene/vinyl acetate copolymer composites." *Journal of Applied Polymer Science*, vol. 107, pp. 2626-2631.
- [4] Duquesne, S., Bras, M. L., Bourbigot, S., Delobel, R., Vezin, H., Camino, G., Eling, B., Lindsay, C., and Roels, T., 2003. "Expandable graphite: A fire retardant additive for polyurethane coatings." *Fire and Materials*, vol. 27, pp. 103-117.
- [5] Zhang, J., Horrocks, A. R., and Hall, M. E., 1994. "The flammability of polyacrylonitrile and its copolymers IV. The flame retardant mechanism of ammonium polyphosphate." *Fire and Materials*, vol. 18, pp. 307-312.
- [6] Lu, C., Cao, Q. Q., Hu, X. N., Liu, C. Y., Huang, X. H., and Zhang, Y. Q., 2014. "Influence of morphology and ammonium polyphosphate dispersion on the flame retardancy of polystyrene/nylon-6 blends." *Fire and Materials*, , vol. 38, pp. 765-776.
- [7] Gaan, S., Sun, G., Hutches, K., and Engelhard, M. H., 2008. "Effect of nitrogen additives on flame retardant action of tributyl phosphate: Phosphorus-nitrogen synergism." *Polymer Degradation and Stability*, vol. 93, pp. 99-108.
- [8] Zheng, Z. H., Sun, H. M., Li, W. J., Zhong, S. L., Yan, J. T., Cui, X. J., and Wang, H. Y., 2013. "Co-microencapsulation of ammonium polyphosphate and aluminum hydroxide in halogen-free and intumescent flame retarding polypropylene." *Polymer Composites*, vol. 35, pp. 715-729.
- [9] Ge, L. L., Duan, H. J., Zhang, X. G., Chen, C., Tang, J. H., and Li, Z. M., 2012. "Synergistic effect of ammonium polyphosphate and expandable graphite on flame-retardant properties of acrylonitrile-butadiene-styrene." *Journal of Applied Polymer Science*, vol. 126, pp. 1337-1343.
- [10] Modesti, M., Lorenzetti, A., Simioni, F., and Camino, G., 2002. "Expandable graphite as an intumescent flame retardant in polyisocyanurate polyurethane foams." *Polymer Degradation and Stability*, vol. 77, pp. 195-202.

- [11] Sun, Z. D., Ma, Y. H., Xu, Y., Chen, X. L., Chen, M., Yu, J., Hu, S. C., and Zhang, Z. B., 2014. "Effect of the particle size of expandable graphite on the thermal stability, flammability, and mechanical properties of high-density polyethylene/ethylene vinyl-acetate/expandable graphite composites." *Polymer Engineering & Science*, vol. 54, pp. 1162-1169.
- [12] Shioyam, H. and Fujii, R., 1987. "Electrochemical reactions of stage 1 sulfuric acid-graphite intercalation compound." *Carbon*, vol. 25, pp. 771-774.
- [13] Song, K. M., Lu, W. Y., and Gao, S. Y., 1993. "A method for the preparation of expandable graphite with low sulfur content. CN 93119757.0."
- [14] Song, K. M., Li, G. S., Feng, Y. L., and Yan, Q. Y., 1996. "Preparation of low-sulfur expandable graphite by using mixing acid." *Chinese Journal of Inorganic Materials*, vol. 11, pp. 749-752.
- [15] Pang, X. Y., Tian, Y., and Weng, M. Q., 2015. "Preparation of expandable graphite with silicate assistant intercalation and its effect on flame retardancy of ethylene vinyl acetate composite." *Polymer Composites*, vol. 36, pp. 1407-1416.
- [16] Xu, D. M., Ding, F., Hao, J. W., and Du, J. X., 2013. "Preparation of modified expandable graphite and its flame retardant application in rigid polyurethane foam." *Chemical Journal of Chinese Universities-Chinese*, vol. 34, pp. 2674-2680.
- [17] Lai, Q., Zhu, S. F., Liu, G. Q., Zou, M., and Li, Y. F., 2010. "Preparation and characterization of TiO<sub>2</sub>/expanded graphite." *Transactions of Tianjin University - Chinese*, vol. 16, pp. 156-159.
- [18] Seefeldt, H., Braun, U., and Wagner, M. H., 2012. "Residue stabilization in the fire retardancy of wood-plastic composites: combination of ammonium polyphosphate, expandable graphite, and red phosphorus." *Macromolecular Chemistry and Physics*, vol. 213, pp. 2370-2377.
- [19] Zhao, C., Gu, X. J., Zhong, S. H., and Xiao, X. F., 2004. "Study on the reaction behaviors of forming propylene oxide from 1,2-dichloropane on Fe-Al-P-O catalyst." *Journal of Chemical Engineering of Chinese University*, vol. 18, pp. 510-514.
- [20] Zhang, Y., Chen, X. L., and Fang, Z. P., 2013. "Synergistic effects of expandable graphite and ammonium polyphosphate with a new carbon source derived from biomass in flame retardant ABS." *Journal of Applied Polymer Science*, vol. 128, pp. 2424-2432.